

## Effective ripple for the W7-X magnetic field calculated by the PIES code\*

M. Drevlak<sup>1</sup>, M. F. Heyn<sup>2</sup>, V. N. Kalyuzhnyj<sup>3</sup>, S. V. Kasilov<sup>3</sup>, **W. Kernbichler**<sup>2</sup>,  
D. Monticello<sup>4</sup>, V. V. Nemov<sup>3</sup>, J. Nührenberg<sup>1</sup>, A. Reiman<sup>4</sup>

<sup>1</sup>Max-Planck-Institut für Plasmaphysik, Association EURATOM-IPP  
Greifswald, GERMANY

<sup>2</sup>Institut für Theoretische Physik, Technische Universität Graz  
Association EURATOM-ÖAW, Graz, AUSTRIA

<sup>3</sup>Institute of Plasma Physics, NSC "Kharkov Institute of Physics and Technology",  
Kharkov, UKRAINE

<sup>4</sup> Princeton Plasma Physics Laboratory, Princeton NJ, USA

### Introduction

The PIES code [1] is a 3-dimensional finite beta equilibrium code developed without a priori assumption of nested magnetic surfaces. This code represents the magnetic field in real space coordinates taking into account a finite plasma pressure as well as external currents. Here, results from PIES for the Wendelstein 7-X (W7-X) configuration are used to compute neoclassical transport in the  $1/\nu$  regime. For this purpose, a technique [2] based on the integration along magnetic field lines in a given magnetic field is used.

### Magnetic field presentation

In cylindrical coordinates  $R, \varphi, z$ , the magnetic field calculated by the PIES code can be presented in the following form:

$$B_R = \sum_{m=0}^{m_{max}} \sum_{n=-n_{max}}^{n_{max}} B_{Rmn}(s) \sin(nn_p \varphi - m\theta) \quad (1)$$

$$B_z = \sum_{m=0}^{m_{max}} \sum_{n=-n_{max}}^{n_{max}} B_{zmn}(s) \cos(nn_p \varphi - m\theta) \quad (2)$$

$$B_\varphi = R \sum_{m=0}^{m_{max}} \sum_{n=-n_{max}}^{n_{max}} B_{mn}^\varphi(s) \cos(nn_p \varphi - m\theta) \quad (3)$$

$$R = \sum_{m=0}^{m_{max}} \sum_{n=-n_{max}}^{n_{max}} R_{mn}(s) \cos(nn_p \varphi - m\theta) \quad (4)$$

$$z = \sum_{m=0}^{m_{max}} \sum_{n=-n_{max}}^{n_{max}} z_{mn}(s) \sin(nn_p \varphi - m\theta). \quad (5)$$

Here,  $s, \theta$  and  $\varphi$  give the background coordinate system in which all quantities computed by the PIES code are given,  $n_p$  is the number of field periods (for W7-X  $n_p = 5$ ). The coordinates  $s, \theta$  and  $\varphi$  are real space coordinates. In contrast to magnetic coordinates, the  $s$  value is not constant on a magnetic surface. The decomposition coefficients  $B_{Rmn}$ ,  $B_{zmn}$ ,  $B_{mn}^\varphi$ ,  $R_{mn}$  and  $z_{mn}$  of the spectra (1) - (5) are given in sets of data obtained as

---

\*This work was partly supported by the project INTAS-99-00592, by the Austrian Academy of Sciences and by the Association EURATOM-ÖAW. The content of the publication is the sole responsibility of its publishers and it does not necessarily represent the views of the Commission or its services.

results of a PIES run. The radial dependencies of these coefficients are given in a set of discrete radial mesh points  $s_j = j/j_{max}$ ,  $j = 1, 2, \dots, j_{max}$ . Between mesh points, the decomposition coefficients are computed using cubic splines. The use of splines is also necessary for the computation of spatial derivatives of the magnetic field.

Computations of all quantities considered in this work are carried out in the background coordinate system  $s$ ,  $\theta$  and  $\varphi$ . The necessary coordinate vectors as well as the quantities  $\nabla s$  and  $\nabla\theta$  are calculated on the basis of formulas (4) - (5). For the integration along magnetic field lines, the contra-variant components of  $\mathbf{B}$ ,  $B^s$  and  $B^\theta$ , are necessary. These components can be calculated as  $B^s = \mathbf{B} \cdot \nabla s$  and  $B^\theta = \mathbf{B} \cdot \nabla\theta$ . It is necessary to note that the contra-variant components of  $\mathbf{B}$  are also obtained directly from the PIES data. In particular, the  $B_{m,n}^\varphi(s)$  decomposition coefficients in formula (3) represent the contra-variant component  $B^\varphi$ .

### Effective ripple and $1/\nu$ neoclassical transport

It is well known that for the  $1/\nu$  transport regime the characteristic features of the specific magnetic field geometry manifest themselves in particle and heat fluxes through the factor  $\epsilon_{\text{eff}}^{3/2}$ , where  $\epsilon_{\text{eff}}$  is the so-called effective ripple. For a conventional stellarator,  $\epsilon_{\text{eff}}$  coincides with the helical ripple  $\epsilon_h$ . For the magnetic field of an arbitrary stellarator, the quantity  $\epsilon_{\text{eff}}^{3/2}$  can be calculated [2] with the help of the following expression:

$$\epsilon_{\text{eff}}^{3/2} = \frac{\pi R_0^2}{8\sqrt{2}} \lim_{L_s \rightarrow \infty} \left( \int_0^{L_s} \frac{ds}{B} \right) \left( \int_0^{L_s} \frac{ds}{B} |\nabla\psi| \right)^{-2} \int_{B_{\min}^{\text{abs}}/B_0}^{B_{\max}^{\text{abs}}/B_0} db' \sum_{j=1}^{j_{\max}} \frac{\hat{H}_j^2}{\hat{I}_j}, \quad (6)$$

$$\hat{H}_j = \frac{1}{b'} \int_{s_j^{\min}}^{s_j^{\max}} \frac{ds}{B} \sqrt{b' - \frac{B}{B_0}} \left( 4 \frac{B_0}{B} - \frac{1}{b'} \right) |\nabla\psi| k_G, \quad \hat{I}_j = \int_{s_j^{\min}}^{s_j^{\max}} \frac{ds}{B} \sqrt{1 - \frac{B}{B_0 b'}}. \quad (7)$$

Here,  $R_0$  is the major radius of the torus,  $B_0$  is a reference magnetic field,  $\psi$  is the magnetic surface label,  $k_G = (\mathbf{h} \times (\mathbf{h} \cdot \nabla)\mathbf{h}) \cdot \nabla\psi / |\nabla\psi|$  is the geodesic curvature of a magnetic field line with the unit vector  $\mathbf{h} = \mathbf{B}/B$ ,  $s$  is the magnetic field line length (and not the radial coordinate  $s$  of the background coordinate system in formulas (1) - (5)).

The quantity  $\epsilon_{\text{eff}}$  is calculated by integration over the magnetic field line length,  $s$ , over the sufficiently large interval  $0 \div L_s$ , and by integration over the perpendicular adiabatic invariant of trapped particles,  $J_\perp$ , by means of the variable  $b'$ . Here,  $B_{\min}^{\text{abs}}$  and  $B_{\max}^{\text{abs}}$  are the minimum and maximum values of  $B$  within the interval  $0 \div L_s$ . The quantities  $s_j^{\min}$  and  $s_j^{\max}$  within the sum over  $j$  in (6) - (7) correspond to the turning points of trapped particles.

In accordance with [2], formulas (6) - (7) must be supplemented with the magnetic field line equations as well as with equations for the vector  $\mathbf{P} \equiv \nabla\psi$

$$\frac{dP_i}{ds} = -\frac{1}{B} \frac{\partial B^j}{\partial \xi^i} P_j, \quad (8)$$

where  $B^j$  are the contra-variant components of  $\mathbf{B}$  in real-space coordinates  $\xi^i$ , and  $P_j = \partial\psi/\partial\xi^j$  are the covariant components of  $\mathbf{P}$ .

## Computational results

Here, results for three different cases are presented. The reference case is a free boundary equilibrium for the W7-X standard high-mirror configuration with  $\langle \beta \rangle = 1\%$  ( $m_{max} = 20$ ,  $n_{max} = 18$  and  $j_{max} = 100$  in Eqs. (1) - (5)). For comparison, a zero  $\beta$  case is also considered using both, PIES data ( $m_{max} = 18$ ,  $n_{max} = 16$  and  $j_{max} = 80$ ) as well as currents in modular coils where the magnetic field is computed with the help of the Biot-Savart law.

Figure 1 shows some results for magnetic surfaces in the  $\varphi = 0$  plane obtained as results of PIES runs. For the  $\beta = 0$  case, curves 1 and 3 show results for the outermost magnetic surface and for some inner magnetic surface, respectively. In the region inside curve 1, magnetic surfaces for this case practically coincide with magnetic surfaces for the vacuum magnetic field. For the  $\beta = 0.01$  case, the outermost magnetic surface (curve 2 in Figure 1) is a little smaller than the corresponding surface for the  $\beta = 0$  case. In addition, magnetic surfaces for the  $\beta = 0.01$  case are somewhat shifted to the outside of the torus. Also note that the outermost magnetic surfaces obtained with the PIES code differ from the starting boundary surface for the free-boundary run (curve 5 in Figure 1).

Results of  $\epsilon_{eff}^{3/2}$  computations are shown in Figure 2. These results are presented as functions of the ratio  $r/a$  where  $r$  is the mean radius of a given magnetic surface and  $a$  is the mean radius of the pertinent outermost magnetic surface shown in Figure 1. From Figure 2 follows that in the region where both data exist,  $\epsilon_{eff}^{3/2}$  values are almost identical for both  $\beta = 0$  cases (PIES and modular coils). Computations for the  $\beta = 0.01$  case reveal a small decrease of  $\epsilon_{eff}^{3/2}$  as compared to the  $\beta = 0$  case.

For a conventional stellarator with an equivalent size, the  $\epsilon_{eff}^{3/2}$  value is within the limits  $0.01 \div 0.03$ . For significant parts of the magnetic configurations produced by the PIES code,  $\epsilon_{eff}^{3/2}$  turns out to be in the limits of  $0.0022 \div 0.0035$ . These values are essentially smaller than those for a conventional stellarator. However, it should be noted that these values are approximately two times bigger than the corresponding values of  $\epsilon_{eff}^{3/2}$  which were found for the W7-X configurations obtained as results of equilibrium runs with a fixed boundary [3].

## Summary

The evaluation of neoclassical transport coefficients in the  $1/\nu$  regime is an important task in stellarator optimization. The technique based on integration along magnetic field lines [2] can be efficiently used to study transport properties of different equilibria. One unique feature of the method is the possibility of a direct evaluation of magnetic configurations.

In this paper, results of effective ripple computations are given for two free boundary equilibria resulting from PIES runs and for a vacuum magnetic field directly produced by modular coils. As expected, the results for the zero  $\beta$  PIES case are almost identical to the results for the vacuum magnetic field computed from coil currents. In almost the whole confinement region the values of the  $\epsilon_{eff}^{3/2}$  parameter turn out to be in the limits of  $0.0022 \div 0.0035$ . This gives  $\epsilon_{eff}$  values in the range from 1.7% to 2.3%. The presence of a plasma in the finite  $\beta = 1\%$  case improves the results slightly throughout the whole region. Compared to a conventional stellarator with equivalent size, the results for  $\epsilon_{eff}^{3/2}$

turn out to be significantly smaller. Compared to prior results for a W7-X equilibrium with a fixed boundary,  $\epsilon_{\text{eff}}^{3/2}$  results for the free boundary equilibria turn out to be roughly a factor 2 higher. Another interesting fact is the big and rather sharp increase of  $\epsilon_{\text{eff}}^{3/2}$  in the close vicinity of the outermost magnetic surface.

### References

- [1] A. H. Reiman and H. S. Greenside, *J. Comput. Phys.* **75**, 423 (1988).
- [2] V. V. Nemov, S. V. Kasilov, W. Kernbichler and M. F. Heyn, *Phys. Plasmas* **6**, 4622 (1999).
- [3] V. V. Nemov, S. V. Kasilov, C. Nührenberg, J. Nührenberg, W. Kernbichler and M. F. Heyn, *Plasma Phys. Control. Fusion* **45**, 43 (2003).

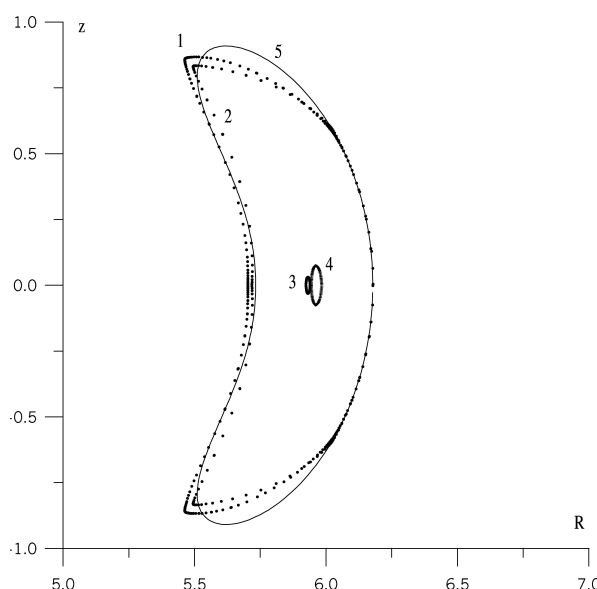


Fig. 1: Outermost and inner magnetic surfaces for magnetic fields obtained as results of PIES runs for  $\beta = 0$  (curves 1 and 3) and for  $\beta = 0.01$  (curves 2 and 4), resp.. Curve 5 shows the starting boundary surface for the free boundary run in the  $\beta = 0$  case.

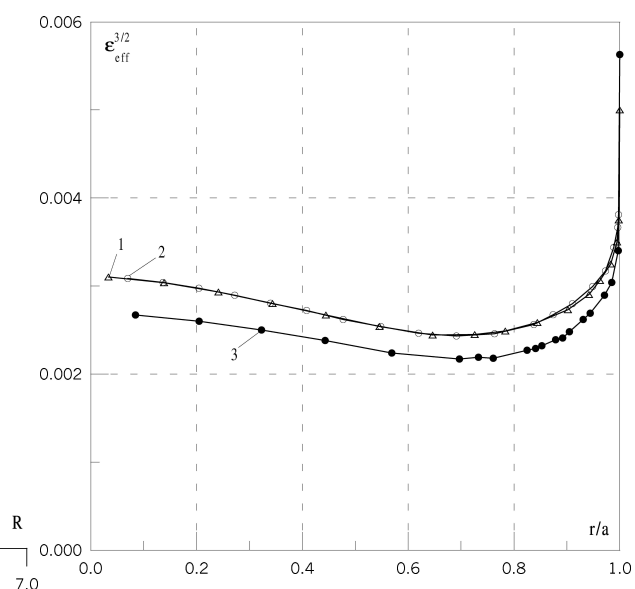


Fig. 2: Parameter  $\epsilon_{\text{eff}}^{3/2}$  for a magnetic field produced by modular coils (curve 1 marked by triangles) and for fields produced as results of PIES runs for  $\beta = 0$  (curve 2 marked by circles) and  $\beta = 0.01$  (curve 3).